Organic & Biomolecular Chemistry

Cite this: *Org. Biomol. Chem.*, 2012, **10**, 5049

www.rsc.org/obc

PAPER

Possible cage-like nanostructures formed by amino acids

Cui-hong Wang,[a,b,c] Qi Wu,[a] Wen-jie Fan,[d] Rui-qin Zhang*[a] and Zijing Lin*[b,e]

Received 15th March 2012, Accepted 6th May 2012
DOI: 10.1039/c2ob25558h

We report possible cage-like nanostructures formed by a representative amino acid, serine octamers and decamers, determined by binding energy calculations and molecular dynamic simulations using the density functional tight-binding method. We used the L-handed serine to construct complex conformers linked by hydrogen bonds. We found the structures linked by –COOH···O═C– to be the most stable conformers and the calculation of the vibrational modes of complexes further illustrated this result. We attempted to apply our cage-like structures to the delivery of C_{20} and cycloserine as model molecules. Our results may shed light on the design of cage-like biocompatible complexes for drug delivery.

Introduction

Because of the insolubility, instability, and toxicity of many drug candidates, self-assembled nanoscale drug delivery systems have recently attracted considerable attention.[1–4] The design and synthesis of novel tubular and cage-like structures to examine their applications as membrane ion channel mimics and hosts have been extensively researched.[5–7] Several packaged drugs use carriers for drug delivery, such as the calyx[6] and the calyx arene derivatives[8] with large cavities. These packages are used because these drugs have specific controlled, sustained, and targeted release characteristics;[8] also, a nanoscale drug delivery system can increase the solubility of the parent drug and maintain the drug's structural integrity.

Amino acids and peptides, the elemental building blocks of proteins, are attracting increasing interest as components for building biological materials.[9–26] There have been many studies on highly constrained amino acids, which is a growing field in molecular modeling and peptide chemistry, since they are useful in constructing peptidomimetics with certain beneficial features for medicinal applications.[9–13] Xin *et al.*[14] used amino acids as linkers in the conjugation of paclitaxel, with hyaluronic acid for the drug delivery system. Raman *et al.*[15] designed a novel type of nanoparticle with regular polyhedral symmetry using peptides. Cooks and colleagues studied the spontaneous formation of a protonated serine octamer by both ion trap tandem mass spectrometry and *ab initio* calculations.[16,17] Many studies have also been carried out on the tube-like structures formed by amino acids.[19–26] The assembled supramolecule can be linked by different interactions, some of which are weak. For example, Lou *et al.* studied the Ala-Gln dipeptide-based supramolecules linked by hydrogen bonds.[27] Fung *et al.*[28] used three self-assembling peptide strategies (hydrogen bonds, and ionic and hydrophobic pairs) to construct a short novel supramolecule that demonstrated the ability to deliver the hydrophobic anticancer agent ellipticine.

The designs of molecules are critical in determining both the properties and functions of the resulting assemblies. Our purpose in this research was to use amino acids to construct cage-like structures that could be used as drug delivery systems. We selected serine, one of the 20 natural amino acids, to form the cage-like structures. Because the most stable conformer of serine is canonical and the zwitterionic is not stable in gas phase, in this research, only the canonical conformers were considered. All structures were optimized by a density functional tight-binding (DFTB) method, complemented by an empirical London dispersion energy term.[29–32] We further analyzed the relative energies, binding energies, and vibrational spectrum of various stable structures. Our work is expected to provide a strategy for constructing supramolecules for nanomedicine applications.

Modeling and computational methods

We used the amino acid L-handed serine as the monomer to construct the cage structure. For the serine monomer, there are three possible hydrogen bond donors and acceptors: the carboxyl (–COOH), the hydroxyl (–OH), and the amino group ($–NH_2$). In our work, the serine molecule was grouped into four parts: the carboxyl (–COOH) is the first part (A), the hydroxyl (–OH) is the second part (B), the amino group ($–HN_2$) is the third part (C) and the remainder forms the fourth group. The illustration of the

[a]*Department of Physics and Materials Sciences, City University of Hong Kong, Hong Kong SAR, China. E-mail: aprqz@cityu.edu.hk*
[b]*Department of Physics, University of Science and Technology of China, Hefei 230026, China. E-mail: zjlin@ustc.edu.cn*
[c]*USTC-CityU Joint Advanced Research Centre, Suzhou 215123, China*
[d]*State Key Laboratory of Molecular Dynamics, Dalian Institute of Chemical Physics, Chinese Academy of Sciences, Dalian 116023, P.R. China*
[e]*Hefei National Laboratory for Physical Sciences at the Microscale, University of Science and Technology of China, Hefei 230026, China*

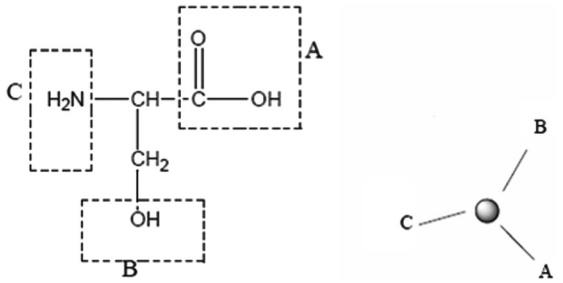

Fig. 1 The illustration of the four parts of serine.

four groups is shown in Fig. 1. There are both hydrogen and electronegative atoms in each of the A, B, and C groups. Each group may act as either hydrogen bond donor or acceptor for forming the intramolecular or intermolecular hydrogen bonds.[33,34] In this work, the formation of a hydrogen bond is judged by geometric criteria with a cut-off of 2.8 Å for the donor and acceptor distance.

We built the cage-like complex using a serine octamer. Since there are three groups of hydrogen bond donors and acceptors for a serine monomer, four types of initial trial conformers could be constructed:

Type (a): H bonds between –OH and –NH_2, and H bonds between –COOH and –COOH (Fig. 2a);

Type (b): H bonds between –COOH and –OH, and H bonds between –NH_2 and –NH_2 (Fig. 2b);

Type (c): H bonds between –COOH and –NH_2, and H bonds between –OH and –OH (Fig. 2c); and

Type (d): H bonds between the –COOH, –NH_2, and –OH, respectively (Fig. 2d).

We designed all of these four kinds of complex by the rotation of the bond angles of the serine and then all the trial complexes were used in the investigation.

Hydrogen bonds play a significant role in stabilizing the structures of the cage-like complexes. For relatively large complexes with 112–160 atoms, we used a computationally efficient approximation to density functional theory (DFT), the self-consistent-charge density-functional tight-binding (SCC-DFTB) scheme, complemented by an empirical London dispersion energy term (acronym DFTB-D). The DFTB-D scheme has been found reliable for predicting the geometrical structure and binding energy of weak interaction systems. For example, in the report of Lin *et al.*,[35] the mean O–O distance of water dimer, trimer, tetramer, and pentamer predicted by DFTB-D is in good agreement with those obtained with the MP2 and CCSD(T) methods. In a number of testing calculations of other structures, our calculated length of hydrogen bond of a formic acid dimer is 1.69 Å by DFTB-D, which compared well with the 1.67 Å, 1.69 Å, 1.69 Å, and 1.68 Å from B3LYP, BH and HLYP, M06L and MP2 calculations with the basis set 6-311++G(2df,2p), respectively. A comprehensive description of the method can be found in the literature.[29–32]

We optimized the conformers using the conjugate gradient algorithm until the residual forces were below 10^{-4} au, and set the charge convergence criterion at 10^{-5} electrons. The most stable conformer was defined as the structure with the lowest total energy after the optimization. We used the same method for cage-like structures formed by a serine decamer. We found that

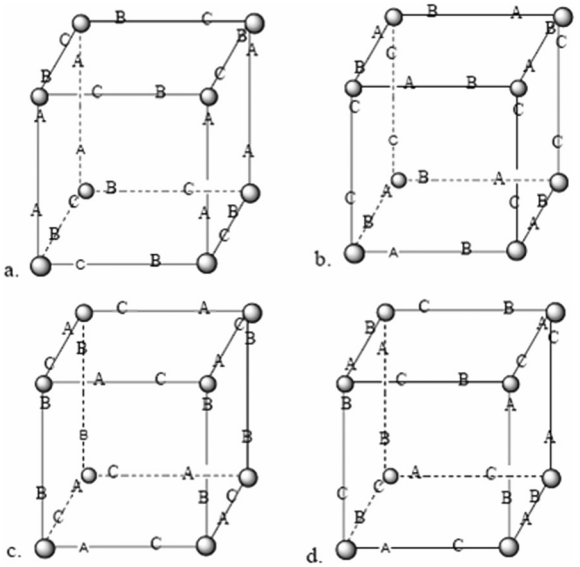

Fig. 2 Four kinds of possible conformers constructed by a serine octamer; all complexes are linked by hydrogen bonds.

Table 1 Relative energies (ΔE), binding energies per unit (E_b), and critical temperature (T_c) of the cage-like structures

Name	ΔE (kcal mol^{-1})	E_b (kcal mol^{-1})	T_c (K)
$(L\text{-}S)_{8a}$	0.00	12.91	500
$(L\text{-}S)_{8c}$	33.01	8.67	350
$(L\text{-}S)_{10}$-1	0.00	12.77	450
$(L\text{-}S)_{10}$-2	1.98	12.71	450
$(L\text{-}S)_{10}$-3	2.07	12.68	450
$(L\text{-}S)_{10}$-4	5.34	12.59	420
S_{10}-C_{20}-1	0.00	27.13	410
S_{10}-C_{20}-2	2.35	24.78	320
S_{10}-Cyc-1	0.00	25.85	320
S_{10}-Cyc-2	5.69	20.16	300

The energies of $(L\text{-}S)_{8a}$, $(L\text{-}S)_{10}$-1, S_{10}-C_{20}-1, and S_{10}-Cyc-1 are set as energy references (0.00 kcal mol^{-1}).

only those molecules linked by a type (a) hydrogen bond (–COOH···O=C–) had stable conformers, and so we did not consider the other three types of structures for the research of the serine decamer. As possible applications for drug delivery, the smallest fullerene, C_{20}, and the small drug molecule, cycloserine, were introduced into the serine decamer cage-like structure, and the complex was optimized using the SCC-DFTB-D scheme.

To further test the structural stability of cage-like structures, we performed a DFTB molecular dynamic simulation by increasing the temperature of the complexes. The temperature was increased 1 K every 100 steps, the simulation time step was set at 1 fs, and constant temperature simulations lasted for 1 ps at the high temperature as listed in Table 1. The charge convergence criterion was set at 10^{-5} electrons. Finally, we calculated and analyzed the vibrational modes of the cage-like complexes, which may be helpful for future experiments. All calculations were performed using the DFTB + 1.1 program.[29–32]

Results and discussion

Stable conformers and their energies

For the serine octamer, we optimized all four types of conformers. The conformer with the lowest total energy was the most stable. After optimization, we found that only the structure of type (a) had a perfect cage-like structure. The other types could not exist stably. Types (b) and (d) collapsed or ruptured, while type (c) changed considerably from the initial structure, leading to a new type of stable cage-like structure.

Fig. 3 shows the most stable cage-like structure of (L-S)$_{8a}$. It is shown in top view and side view. Here "L" refers to L-handed, "S" is the logogram of serine, "8" refers to the cage-like structure formed by an amino acid octamer, and "a" refers to a type (a) structure. The stable cage structures have symmetrical structures. The top view shows hydrogen bonds –OH···OH–, while the side view presents the hydrogen bonds –COOH···O=C–. Fig. 3 also shows the bond lengths of the –COOH···O=C– and –OH···OH– hydrogen bonds. For (L-S)$_{8a}$, the lengths for the –COOH···O=C– and –OH···OH– hydrogen bonds are 1.74 Å and 1.85 Å, respectively.

Fig. 4 presents the structure of (L-S)$_{8c}$, which is the new structure derived from type (c), and the lengths of the hydrogen bonds. To illustrate the structure, two partial views in which the structure has been cut in the center are shown at the bottom. The type (c) structure is more compact than type (a). In the top view, there are two kinds of hydrogen bonds: –OH···OH– bonds and –NH···O=C– bonds, with bond lengths of 1.88 Å and 2.38 Å, respectively. The hydroxyl of the serine is in the side, and leads to the formation of –OH···O=C– bonds of 1.97 Å. The structure (S)$_{8c}$ is less stable than (S)$_{8a}$, although it has more hydrogen bonds. This may be owing to its compact structure, in which the exclusive interactions weaken the hydrogen bonds.

Table 1 shows the relative energies of the (S)$_8$ molecules. The conformers (S)$_{8c}$ have evidently higher energies than (S)$_{8a}$. The energy of (L-S)$_{8a}$ is set as the reference (0.00 kcal mol^{-1}), and the relative energy of (L-S)$_{8c}$ is 33.01 kcal mol^{-1} higher than (L-S)$_{8a}$. When we compared the length of the hydrogen bonds in Fig. 3 and Fig. 4, we found that the lower energy conformer has stronger hydrogen bonds. So, the hydrogen bonds play important roles in stabilizing the structure of serine octamers. We conclude that the (L-S)$_{8a}$ complex containing the –COOH···O=C– hydrogen bonds is the most stable conformer of the four types of initial structures formed by the L-handed serine octamers. Our work is thus consistent with the report of Cooks *et al.*[16] In their report, the calculated HF/6-31G structure of the protonated serine octamer in their Fig. 6 has a –COOH···O=C– hydrogen bond too.

Since the structure of type (a) with –C=O···HOOC– hydrogen bonds is the most stable (S)$_8$ conformer, we constructed the (S)$_{10}$ cage-like structures linked by the same type of hydrogen bonds. Fig. 5 displays the four stable conformers of (L-S)$_{10}$ in top view and side view. They have similar structures to the (S)$_8$ complexes. The top view of the structure is nearly a perfect pentacle. As the lean of the side view of (S)$_{10}$ is smaller than that of (S)$_8$, the (S)$_{10}$ complex is a little "taller" than the (S)$_8$ complex. The main difference of the four stable complexes concerns the orientations of their amino groups and the lengths of the –OH···OH– bonds. Fig. 5 also gives the lengths of the hydrogen bonds. The lengths of the hydrogen bonds, –OH···OH–, are 1.88 Å, 1.90 Å, 1.90 Å and 1.91 Å for (L-S)$_{10}$-1, (L-S)$_{10}$-2, (L-S)$_{10}$-3, and (L-S)$_{10}$-4, respectively. The lengths of the hydrogen bonds –COOH···O=C– are the same at 1.74 Å for all the four (S)$_{10}$ conformers. The hydrogen bonds –OH···OH– in (S)$_{10}$ are longer and weaker than those in the serine octamer.

The relative energies of the four serine decamers are shown in Table 1. The energy of (L-S)$_{10}$-1 is set as the energy reference (0.00 kcal mol^{-1}), and the relative energies of (L-S)$_{10}$-2, (L-S)$_{10}$-3, and (L-S)$_{10}$-4 are 1.98 kcal mol^{-1}, 2.07 kcal mol^{-1} and 5.34 kcal mol^{-1}, respectively.

Stability of the structures

To compare the stability of different cage-like structures, we calculated the binding energies per amino acid using the following equation:

$$E_b = \frac{1}{n}\left(\sum_{i=1}^{n} E_i^0 - E\right) \quad (1)$$

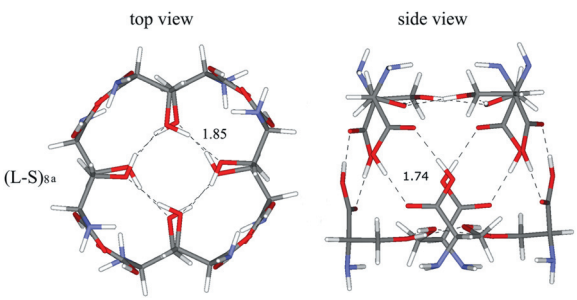

Fig. 3 The stable serine octamer complex (a) constructed by L-serine. They are shown in top view and side view. The number in the figure is the length of the hydrogen bond (Å).

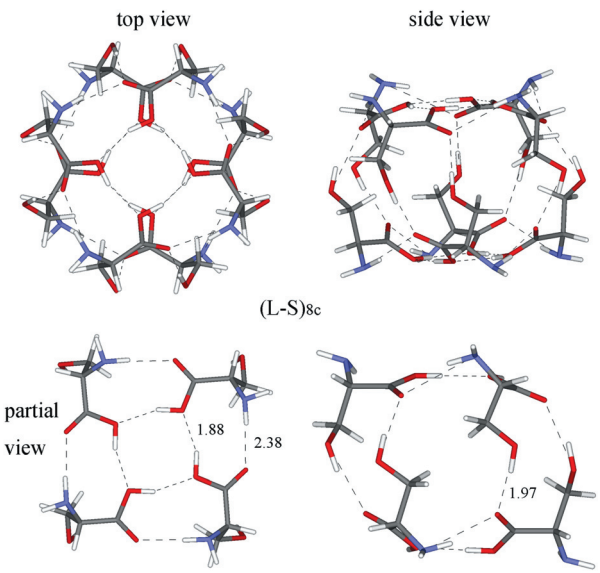

Fig. 4 The new stable serine octamer complexes (c) constructed by L-serine. The two figures at the bottom are partial view structures of (L-S)$_{8c}$; The numbers in the figure are the lengths of the hydrogen bonds (Å).

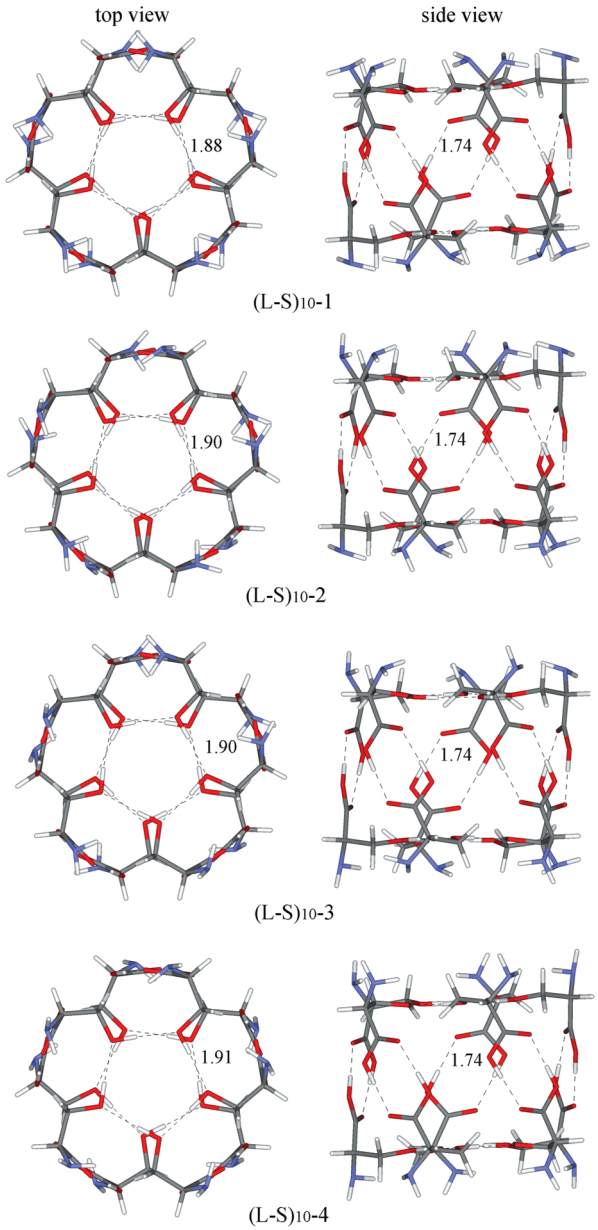

Fig. 5 The stable serine decamer complexes constructed by L-serine. They are shown in top view and side view. The number in the figure is the length of the hydrogen bond (Å).

Here E_i^0 is the serine monomer's energy, E is the complex's energy, and n is the number of serine molecules. Table 1 shows the binding energies per amino acid for the $(S)_8$ and $(S)_{10}$ complexes. For cage-like complexes, the type (a) structures have larger binding energies per unit than type (c). The binding energies demonstrate that the type (a) structure is more stable than type (c). As shown in Table 1, the binding energies of the serine decamers are also larger than $(L\text{-}S)_{8c}$, but are slightly smaller than $(L\text{-}S)_{8a}$.

We further investigated the highest temperature at which the structure remains stable; Table 1 shows the highest temperature for different structures. When we increased the temperature, the cage-like structure would collapse or rupture. $(L\text{-}S)_{8a}$ has the highest stable temperature, and can retain a cage-like structure up to 500 K. For the complexes of $(L\text{-}S)_{8c}$, the maximum temperature is 350 K. For complexes of $(L\text{-}S)_{10}$, the maximum temperatures are 450 K, 450 K, 450 K, and 420 K for conformers 1, 2, 3, and 4, respectively. Our calculations thus show that our cage-like structures are very stable thermally and resistant to collapse, confirming their intrinsically structural rationality. Moreover, the results also show that the thermal stabilities of the structures increase with their hydrogen bond strengths.

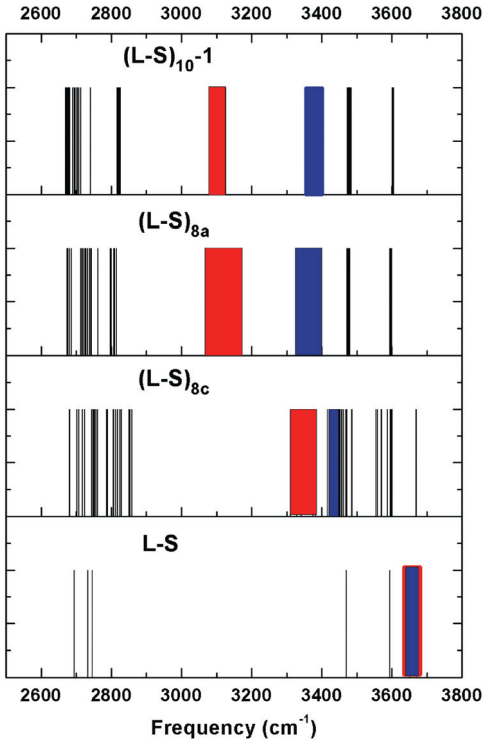

Fig. 6 The vibrational frequency for single serine L-S and complexes $(L\text{-}S)_{8a}$, $(L\text{-}S)_{8c}$, and $(L\text{-}S)_{10}$. This is a representation of the position of the vibrational modes; the height of the line does not denote the intensity of the vibration. The red line is the vibration of the carboxyl hydrogen, and the blue line is the vibration of the hydroxyl hydrogen.

Vibrational frequency analysis of the complexes

We also calculated the vibrational modes of the cage-like structures; Fig. 6 shows the vibrational frequencies for the single serine L-S, $(L\text{-}S)_{8a}$, $(L\text{-}S)_{8c}$, and $(L\text{-}S)_{10}$-1 complexes. Fig. 6 is a representation of the positions of the vibrational modes; the height of the line does not denote the intensity of the vibration. The red line is the vibration of the carboxyl hydrogen, and the blue line is the vibration of the hydroxyl hydrogen. For the L-S monomer, the frequency at the range of 3650 cm^{-1}–3700 cm^{-1} refers to the mixed vibrations of the carboxyl hydrogen and hydroxyl hydrogen. The vibrational frequencies of the carboxyl hydrogen for L-S, $(L\text{-}S)_{8a}$, $(L\text{-}S)_{8c}$, and $(L\text{-}S)_{10}$-1 are in the ranges of 3650 cm^{-1}–3700 cm^{-1}, 3050 cm^{-1}–3200 cm^{-1}, 3300 cm^{-1}–3400 cm^{-1}, and 3050 cm^{-1}–3100 cm^{-1}, respectively. The vibration shows an evident red shift for the serine complex as opposed to the serine monomer. This is further evidence for the existence of the –COOH···O═C– hydrogen bond. It also shows that the red-shift for $(L\text{-}S)_{8a}$ is larger than that for $(L\text{-}S)_{8c}$, further

illustrating that the hydrogen bonds in the type (a) serine octamer and decamer complexes are stronger than those in the type (c) octamer. Because the –COOH···O═C– hydrogen bonds are 1.74 Å for both $(\text{L-S})_{8a}$ and $(\text{L-S})_{10}$-1, they have similar strengths and similar red shifts. The vibrational frequencies of the hydroxyl hydrogen for L-S, $(\text{L-S})_{8a}$, $(\text{L-S})_{8c}$, and $(\text{L-S})_{10}$-1 are in the 3650 cm^{-1}–3700 cm^{-1}, 3300 cm^{-1}–3400 cm^{-1}, 3400 cm^{-1}–3500 cm^{-1}, and 3350 cm^{-1}–3400 cm^{-1} ranges, respectively. The evident red shifts also illustrate the existence of hydrogen bonds, while the $(\text{L-S})_{8c}$ complex has weaker hydroxyl hydrogen bonds than the other two complexes and the latter two complexes have similar hydrogen bond strengths. These results are consistent with the binding energies shown in Table 1.

Possible applications

We further explored the possible application of our cage-like structures in nanoscale drug delivery. Considering the small size of our complex, the smallest fullerene, C_{20}, was used as a model drug molecule and was inserted into the cage-like structure $(\text{L-S})_{10}$-1. After optimization, we found that the complexes of C_{20} surrounded by the $(S)_{10}$ cage-like structure were very stable. There were two stable structures for the L-handed S_{10}-C_{20} complex, respectively, as shown in Fig. 7. They are shown in top view and side view. The complex S_{10}-C_{20}-1 is more stable than the complex S_{10}-C_{20}-2. Table 1 shows the relative energies of the serine decamer-C_{20} complexes. The energy of $(\text{L-S})_{10}$-C_{20}-1 was set as the reference (0.00 kcal mol^{-1}). The energy of complex S_{10}-C_{20}-2 is 2.35 kcal mol^{-1} higher than complex S_{10}-C_{20}-1.

The bond lengths of hydrogen bonds are shown in Fig. 7 too. Comparing the bond lengths of the $(S)_{10}$-C_{20} complexes with those of the $(S)_{10}$ complex, the lengths of –OH···OH– bonds are 2.10 Å, 2.11 Å and 1.90 Å, and the lengths of –COOH···O═C– bonds are 1.76 Å, 1.76 Å and 1.74 Å for S_{10}-C_{20}-1, S_{10}-C_{20}-2 and $(\text{L-S})_{10}$ respectively. It indicates that the hydrogen bonds in the $(S)_{10}$ complex are slightly weaker after interacting with the C_{20} molecule.

We also calculated the binding energies of the amino acid-C_{20} complexes using the equation:

$$E_b = E(S_{10}) + E(C_{20})E(S_{10} - C_{20}) \quad (2)$$

where $E(S_{10})$ is the total energy of the serine decamer, $E(C_{20})$ is the total energy of the C_{20} molecule, and $E(S_{10}\text{-}C_{20})$ is the total energy of the serine decamer-C_{20} complex. The binding energies of S_{10}-C_{20} complexes are shown in Table 1. Our results show that the binding energy of complex 2 is 2.35 kcal mol^{-1} smaller than complex 1, further indicating the greater stability of structure S_{10}-C_{20}-1, compared to S_{10}-C_{20}-2. In Table 1, the highest temperatures at which the structures of the S_{10}-C_{20} complexes 1 and 2 are retained are 410 K and 320 K, respectively. Our calculations thus show that the complexes are very stable. So use of the cage-like structures in drug delivery is possible. Note that Schinazi *et al.* have found that water-soluble fullerene has selective activity against human immunodeficiency virus (HIV) types 1 and 2 *in vitro* and that it shows anti-human immunodeficiency virus protease activities.[36,37] However, the toxicities of fullerene derivatives need to be studied further.[38]

Cycloserine (Cyc) is an antibiotic against mycobacterium avium complex and tuberculosis.[39] It is toxic to enteric bacteria and other eubacteria and is usually used as a second-line drug. The conformer of Cyc is shown in Fig. 8. We put a Cyc molecule into the cage like structure $(\text{L-S})_{10}$-1. The two most stable conformers of S_{10}-Cyc are shown in Fig. 9. For better clarity, the Cyc is highlighted in yellow in the side views. The average length of –OH···OH– bonds are 1.88 Å and 1.92 Å for conformers 1 and 2, respectively. Because of the influence of oxygen and nitrogen atoms in the Cyc molecule, there are three hydrogen bonds between Cyc and the cage structure, and the lengths of –COOH···O═C– bonds are quite different. Conformers 1 and 2 can be understood as parallel and vertical to the cage structures, respectively. The relative energies and binding energies are shown in Table 1. The energy of complex 2 is 5.69 kcal mol^{-1} higher than that of complex 1 and the binding energies of these complexes are respectively 25.85 kcal mol^{-1} and 20.16 kcal mol^{-1}, which are smaller than the S_{10}-C_{20} complexes. The highest temperatures in which the cage structures remain stable are 320 K and 300 K, respectively. Overall, the S_{10}-Cyc complex is influenced by asymmetrical interaction between the

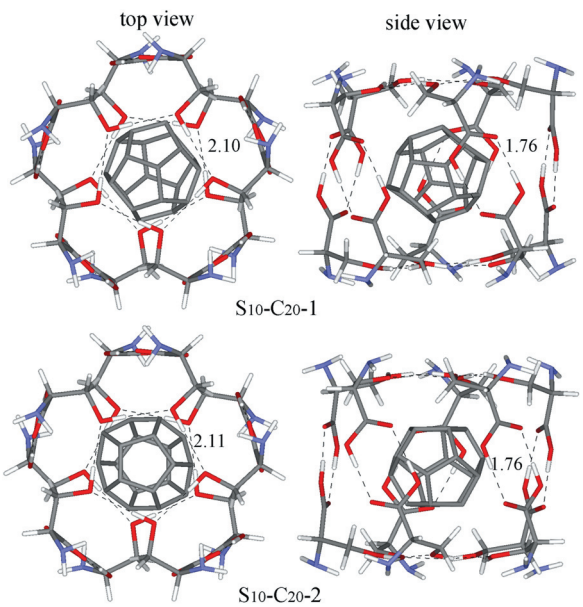

Fig. 7 The stable $(\text{L-S})_{10}$-1-C_{20} complexes constructed by L-serine. They are shown in top view and side view. The numbers in the figure are the lengths of the hydrogen bonds (Å).

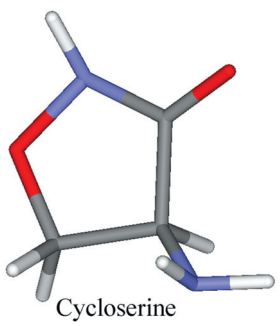

Fig. 8 The conformer of cycloserine.

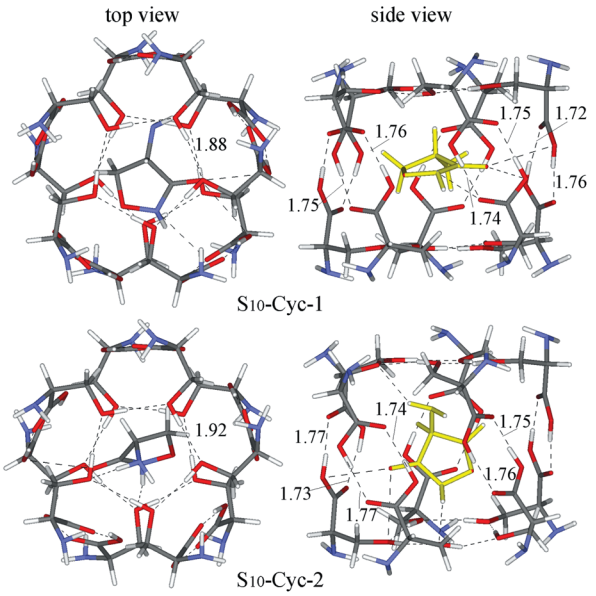

Fig. 9 The stable serine decamer-cycloserine complexes constructed with L-serine monomers. The yellow molecule in the side view is cycloserine. The numbers in the figure are the lengths of the hydrogen bonds (Å).

polar groups of Cyc and the cage structure is less stable than the S_{10}-C_{20} complex.

Conclusions

The most stable cage-like structure formed by the serine octamer is symmetric and linked by –C═O···HOOC– hydrogen bonds. The vibrational-mode calculations further illustrated the existence of hydrogen bonds. The insertions of the smallest fullerene, C_{20}, and cycloserine into the serine decamer cage demonstrate good stability of the cage-like structure for drug delivery applications. Our results may thus be helpful for designing cage-like biocompatible structures for nanoscale drug delivery applications.

Acknowledgements

The work described in this paper was supported by grants from the Research Grants Council of Hong Kong SAR (Project Nos. CityU 103511 and CityU6/CRF/08) and from the National Science Foundation of China (Project No. 11074233), and by the Centre for Applied Computing and Interactive Media (ACIM) of the City University of Hong Kong.

Notes and references

1 R. Haag, *Angew. Chem., Int. Ed.*, 2004, **43**, 278–282.
2 Y. Bae, S. Fukushima, A. Harada and K. Kataoka, *Angew. Chem., Int. Ed.*, 2003, **42**, 4640–4643.
3 J. Li, X. Ni and K. W. Leong, *J. Biomed. Mater. Res.*, 2003, **65**, 196–202.
4 M. T. Morgan, M. A. Carnahan, C. E. Immoos, A. A. Ribeiro, S. Finkelstein, S. J. Lee and M. W. Grinstaff, *J. Am. Chem. Soc.*, 2003, **125**, 15485–15489.
5 G. Pattenden and T. Thompson, *Chem. Commun.*, 2001, 717–718.
6 F. Corbellini, R. M. A. Knegtel, P. D. J. Grootenhuis, M. Crego-Calama and D. N. Reinhoudt, *Chem.–Eur. J.*, 2005, **11**, 298–307.
7 A. Casnati, F. Sansone and R. Ungaro, *Acc. Chem. Res.*, 2003, **36**, 246–254.
8 G. H. Sagar, M. A. Arunagirinathan and J. R. Bellare, *Indian. J. Exp. Biol.*, 2007, **45**, 133–159.
9 A. Cordomi, J. Gomez-Catalan, A. I. Jimenez, C. Cativiela and J. J. Perez, *J. Pept. Sci.*, 2002, **8**, 253–266.
10 K. Van Rompaey, I. Van den Eynde, N. De Kimpe and D. Tourwe, *Tetrahedron*, 2003, **59**, 4421–4432.
11 J. Gomez-Catalan, C. Aleman and J. J. Perez, *Theor. Chem. Acc.*, 2000, **103**, 380–389.
12 J. Gomez-Catalan, A. I. Jimenez, C. Cativiela and J. J. Perez, *J. Pept. Res.*, 2001, **57**, 435–446.
13 R. Kaul and P. Balaram, *Bioorg. Med. Chem.*, 1999, **7**, 105–117.
14 D. Xin, Y. Wang and J. Xiang, *Pharm. Res.*, 2010, **27**, 380–389.
15 S. Raman, G. Machaidze, A. Lustig, U. Aebi and P. Burkhard, *Nanomed.: Nanotechnol., Biol. Med.*, 2006, **2**, 95–102.
16 R. G. Cooks, D. Zhang and K. J. Koch, *Anal. Chem.*, 2001, **73**, 3646–3655.
17 S. C. Nanita and R. G. Cooks, *Angew. Chem., Int. Ed.*, 2006, **45**, 554–569.
18 R. Hodyss, R. R. Julian and J. L. Beauchamp, *Chirality*, 2001, **13**, 703–706.
19 F. Dehez, M. Tarek and C. Chipot, *J. Phys. Chem. B*, 2007, **111**, 10633–10635.
20 H. Hwang, G. C. Schatz and M. A. Ratner, *J. Phys. Chem. A*, 2009, **113**, 3717–3724.
21 E. Khurana, S. O. Nielsen, B. Ensing and M. L. Klein, *J. Phys. Chem. B*, 2006, **110**, 18965–18972.
22 H. Hwang, G. C. Schatz and M. A. Ratner, *J. Phys. Chem. B*, 2006, **110**, 26448–26460.
23 M. Engels, D. Bashford and M. R. Ghadiri, *J. Am. Chem. Soc.*, 1995, **117**, 9151–9158.
24 H. S. Kim, J. D. Hartgerink and M. R. Ghadiri, *J. Am. Chem. Soc.*, 1998, **120**, 4417–4424.
25 L. Delemotte, F. Dehez, W. Treptow and M. Tarek, *J. Phys. Chem. B*, 2008, **112**, 5547–5550.
26 M. R. Ghadiri, J. R. Granja and L. K. Buehler, *Nature*, 1994, **369**, 301–304.
27 B. Lou, X. Huang and Q. Lin, *Z. Anorg. Allg. Chem.*, 2010, **636**, 2539–2542.
28 S. Fung, H. Yang, P. Sadatmousavi, Y. Sheng, T. Mamo, R. Nazarian and P. Chen, *Adv. Funct. Mater.*, 2011, **21**, 2456–2464.
29 G. Seifert, D. Porezag and Th. Frauenheim, *Int. J. Quantum Chem.*, 1996, **58**, 185–192.
30 M. Elstner, D. Porezag, G. Jungnickel, J. Elsner, M. Haugk, T. Frauenheim, S. Suhai and G. Seifert, *Phys. Rev. B: Condens. Matter*, 1998, **58**, 7260–7268.
31 A. K. Rappe, C. J. Casewit, K. S. Colwell, W. A. Goddard III and W. M. Skiff, *J. Am. Chem. Soc.*, 1992, **114**, 10024–10035.
32 M. Elstner, T. Frauenheim and S. Suhai, *THEOCHEM*, 2003, **632**, 29–41.
33 R. Custelcean and J. E. Jackson, *Chem. Rev.*, 2001, **101**, 1963–1980.
34 G. Vogt, S. Woell and P. Argos, *J. Mol. Biol.*, 1997, **269**, 631–643.
35 C. S. Lin, R. Q. Zhang, S. T. Lee, M. Elstner, Th. Frauenheim and L. J. Wan, *J. Phys. Chem. B*, 2005, **109**, 14183–14188.
36 R. F. Schinazi, R. Sijbesma, G. Srdanov, C. L. Hill and F. Wudl, *Antimicrob. Agents Chemother.*, 1993, **37**, 1707–1710.
37 P. Rajagopalan, F. Wudl, R. F. Schinazi and F. D. Boudinot, *Antimicrob. Agents Chemother.*, 1996, **40**, 2262–2265.
38 X. Yan, B. Shi, D. Wang and H. Tang, *Prog. Chem.*, 2008, **20**, 422–428.
39 S. David, *J. Antimicrob. Chemother.*, 2001, **47**, 203–206.

